Title

Cardiac Magnetic Resonance Assessment of Response to Cardiac Resynchronization Therapy and Programming Strategies.

Journal

JACC: Cardiovascular Imaging, 14(12)

Authors

Gao, Xu

Abdi, Mohamad

Auger, Daniel

et al.

Publication Date

2021-12-01

DOI

10.1016/j.jcmg.2021.06.015

Peer reviewed

Published in final edited form as:

JACC Cardiovasc Imaging. 2021 December ; 14(12): 2369–2383. doi:10.1016/j.jcmg.2021.06.015.

Cardiac Magnetic Resonance Assessment of Response to Cardiac Resynchronization Therapy and Programming Strategies

Xu Gao, MD[1], **Mohamad Abdi, MS**[2], **Daniel A. Auger, PhD**[2], **Changyu Sun, PhD**[2], **Christopher A. Hanson, MD**[1], **Austin A. Robinson, MD**[1], **Christopher Schumann, MD**[1], **Pim J. Oomen, PhD**[2], **Sarah Ratcliffe, PhD**[4], **Rohit Malhotra, MD**[1], **Andrew Darby, MD**[1], **Oliver J. Monfredi, MD, PhD**[1], **J. Michael Mangrum, MD**[1], **Pamela Mason, MD**[1], **Sula Mazimba, MD**[1], **Jeffrey W. Holmes, MD, PhD**[2], **Christopher M. Kramer, MD**[1,3], **Frederick H. Epstein, PhD**[2,3], **Michael Salerno, MD, PhD**[2,3], **Kenneth C. Bilchick, MD, MS**[1]

[1]Department of Medicine, University of Virginia Health System, Charlottesville, Virginia

[2]Department of Biomedical Engineering, University of Virginia Health System, Charlottesville, Virginia

[3]Department of Radiology and Medical Imaging, University of Virginia Health System, Charlottesville, Virginia

[4]Department of Public Health Sciences, University of Virginia Health System, Charlottesville, Virginia

Abstract

Background: CMR with cardiac implantable electronic devices can safely provide high-quality right/left ventricular ejection fraction (RVEF/LVEF) assessments and strain.

Objectives: The objective was to determine the feasibility and effectiveness of CMR cine and strain imaging before and after cardiac resynchronization therapy (CRT) for assessment of response and the optimal resynchronization pacing strategy.

Methods: CMR with cine imaging, displacement encoding with stimulated echoes (DENSE) for the CURE-SVD dyssynchrony parameter, and scar assessment was performed before and after CRT. While the pre-CRT scan constituted a single “imaging set” with complete volumetric, strain, and scar imaging, multiple imaging sets with complete strain and volumetric data were obtained during the post-CRT scan for biventricular pacing (BIVP), left ventricular pacing (LVP), and asynchronous atrial pacing modes by reprogramming the device outside the scanner between imaging sets.

Address for Correspondence: Kenneth Bilchick, MD, MS, UVA Health System, Cardiovascular Division, P.O. Box 800158 Charlottesville, VA 22908, tel 434-924-2465, fax 815-346-5805, bilchick@virginia.edu.

Results: 100 CMRs with a total of 162 imaging sets were performed in 50 patients (median age 70 years [IQR 50 to 86 years]; 48% female). Reduction of LV end-diastolic volumes (p=0.002) independent of CRT pacing was more prominent than corresponding reductions in RV end-diastolic volumes (p=0.16). A clear dependence of the optimal CRT pacing mode (BIVP vs LVP) on the PR interval (p=0.0006) was demonstrated. The LVEF and RVEF improved more with BIVP than LVP with PR intervals ≥ 240 ms (p=0.025 and p=0.002, respectively); the optimal mode (BIVP v. LVP) was variable with PR intervals < 240 ms. A lower pre-CRT DENSE CURE-SVD was associated with greater improvements in the post-CRT CURE-SVD (r=−0.69; p<0.001), LVESV (r=−0.58; p<0.001), and LVEF (r=−0.52; p<0.001).

Conclusion: CMR evaluation with assessment of multiple pacing modes during a single scan after CRT is feasible and provides useful information for patient care with respect to response and the optimal pacing strategy.

Keywords

magnetic resonance imaging; heart failure; cardiac resynchronization therapy; implantable cardioverter defibrillator

Introduction

While CRT continues to be a frequently used therapy based on clinical trials (1,2) and guidelines (3) for many patients with chronic systolic heart failure (4), response rates in studies of patients receiving CRT based on these guidelines in clinical practice continue to be approximately 60% and often lower (5). Approaches to improve CRT response have included CRT programming algorithms designed to improve atrioventricular timing and minimize right ventricular (RV) pacing during CRT pacing (6–8); however, it has been challenging to demonstrate differences in volumes and function among pacing algorithms, and it has been hypothesized that this may be due, in part, to the need for a very reproducible imaging approach with a high signal-to-noise ratio. While echocardiography is most often used to assess left ventricular (LV) function after CRT based on volumetric measures and has the advantage of being perhaps the most accessible way to assess LV function, image quality can be highly variable among patients with challenges in defining endocardial borders on long-axis images.

With the now widespread use of MR-conditional CRT defibrillators and evidence establishing safety of MRI in patients with both MR-conditional and non-MR-conditional devices based on large clinical series (9) and expert consensus recommendations (10), CMR is now a safe approach that could yield important data regarding CRT response and programming strategies in patients with CRT defibrillators, particularly with methods capable of high-quality post-device images with minimal artifact (11). In addition, CMR is considered by many to be the standard for RV and LV volumetric and strain imaging. The potentially high reproducibility and image quality achieved with CMR could be very useful clinically for accurate assessments of RV and LV functional changes after CRT. CMR strain imaging in conjunction with biventricular volumetric imaging could also provide important data on mechanisms of CRT response and provide the reproducibility needed to resolve the effects of different CRT programming strategies; however, the feasibility of a post-CRT

imaging approach based on assessments of multiple pacing modes during a single scan is poorly described. These considerations served as the scientific premise for the present study designed to test the hypotheses that assessment of CRT response and the CRT programming strategy with CMR is feasible, and such an approach could provide personalized information for patient care in heart failure.

Methods

Study Design and Informed Consent

Patients at the University of Virginia Health System undergoing CRT-D were enrolled in a prospective study evaluating the use of CMR before and after CRT to evaluate mechanisms of response and programming strategies. All patients provided informed consent for this cohort study, which was approved by the Institutional Review Board for Human Subjects Research at our institution.

Inclusion and Exclusion Criteria

Participants were required to have chronic systolic HF, LVEF ≤ 35%, and a guideline-based class I or IIa indication for CRT (3). Patients were also between 25 and 85 years old, consistent with populations enrolled in CRT trials, and standard exclusion criteria based on CMR were applied.

Study Procedures

Prior to CRT, patients had a contrast-enhanced cardiac magnetic resonance imaging exam and an echocardiogram performed, completed a heart failure questionnaire score (Minnesota Living with Heart Failure Questionnaire), completed basic laboratory testing including a B-type natriuretic peptide, and underwent cardiopulmonary exercise testing if possible. Six months after CRT, these tests were repeated to facilitate comparison with the pre-CRT findings.

Pre-CRT CMR Protocol

The CMR was acquired using a 1.5T MR scanner (Aera, Siemens Healthineers, Erlangen, Germany) using a four-channel phased-array radiofrequency coil. The imaging protocol included steady state free precession (SSFP) and gradient echo (GRE) cine imaging, cine Displacement with Stimulated Echoes (DENSE), and late gadolinium enhancement (LGE). SSFP and GRE cine imaging were performed for all LV short-axis slices (6 mm thickness) without gaps and in 3 standard long-axis slices. Cine DENSE was performed in four short-axis planes at basal, two mid-ventricular, and apical levels. Cine DENSE parameters included a temporal resolution of 17 ms, pixel size of 2.8 x 2.8 mm^2, and slice thickness of 8 mm (12). Displacement was encoded in two orthogonal directions and a spiral k-space trajectory was used with six interleaves per image. Other parameters included: field of view 350 x 350 mm^2, displacement encoding frequency ke = 0.1 cycles/mm, flip angle 15°, and echo time = 1.9 msec. Gadobenate dimeglumine 0.10-0.15 mmol/kg (MultiHance, Bracco Diagnostics Inc., NJ) or gadoterate meglumine (Dotarem, Guerbet USA) 0.10-0.15 mmol/kg) was used for LGE imaging. LGE images were acquired for all short-axis slices and 3 standard long-axis slices.

Post-CRT CMR Protocol

The post-CRT exam was again acquired using a 1.5T MR scanner (Aera, Siemens) with the ipsilateral arm raised when possible. The CMR sequences included again SSFP and GRE cine imaging and DENSE. The post-CRT DENSE acquisition was modified to include twelve instead of six spiral interleaves to increase the signal-to-noise ratio during early systole. All patients had electrocardiographic monitoring during the scan based on the protocol for post-device imaging at our institution (10). A device expert (KB or another provider) was present throughout the scan. In most patients, we assessed cine and DENSE imaging with biventricular pacing (BIVP) and synchronized left ventricular pacing (LVP) with the dual-chamber asynchronous mode (DOO). The atrial asynchronous mode (AOO) was used post-CRT in a subset of patients with intact atrioventricular conduction selected based on efficiency of completion of imaging during LVP and BIVP modes; the purpose was to assess possible reductions in LV chamber size without active resynchronization pacing (known as “LV reverse remodeling” or favorable growth). An imaging set was defined as acquisition of complete cine and strain data for a particular state (pre-CRT) or pacing mode (BIVP, LVP, AOO) before removing the patient from the scanner to program a different pacing mode if another imaging set was to be obtained. In this study, there were two to three imaging sets during the post-CRT scan (corresponding to BIVP, LVP, and/or AOO modes) and one complete imaging set during the pre-CRT scan. After the initial imaging set was completed, the MRI technologist disconnected the patient table from the scanner and moved (rolled) it just outside the MRI exam room for reprogramming (Central Illustration). The programming head was then placed on the patient (between the coils and the patient’s chest) and the programming mode was changed to the next pacing mode. The programming head was then removed from the patient, and the patient on the MRI table was then returned to the scanning chamber, the table reconnected to the scanner, and imaging resumed. After the scan, all lead parameters were again rechecked, tachytherapy programming was again programmed on, and CRT pacing parameters were restored to the initial specifications.

Analysis of CMR Images

The Imaging Core Lab performing the analyses included investigators at the University of Virginia (XG, MA, AR, CH, CSch, CSun, and KB). The left and right end-systolic and end-diastolic volumes normalized for body surface area (LVESVI, LVEDVI, RVESVI, RVEDVI) and LV/RV ejection fractions (LVEF/RVEF) were determined using suiteHEART MRI (NeoSoft, USA). Scar was also quantified from LGE images using the same software based on a signal intensity six standard deviations greater than the signal intensity in remote nulled myocardium. Scar mass and percent scar volume were determined. Circumferential strain from 2-dimensional cine DENSE was calculated semiautomatically in 18 segments per slice (13,14). The circumferential uniformity ratio estimate with singular value decomposition (CURE-SVD) was calculated from DENSE circumferential strain as previously described (15). Briefly a rank-1 approximation of the strain matrix was performed using SVD, and the CURE calculation was applied to the rank-1 approximation to compute the CURE-SVD.

All CMR parameters values were obtained based on semi-automatic methods using standard image analysis software. In addition, as all scans were labeled with anonymous participant identifiers, the investigators performing the analyses were blinded at the time of analysis

to patient characteristics included in later aggregate statistical analyses. In addition, the investigators implementing these software-based semi-automatic methods were blinded to previous or subsequent parameter values obtained during separate scans. As certain acquisitions for each of the different post-CRT imaging sets were labeled based on the pacing mode in order to facilitate the subsequent post-scan analyses, investigators analyzing pacing mode-specific parameters during the post-CRT scan were not technically blinded to the pacing mode; however, it is unlikely that this had a significant influence on the parameter values obtained semiautomatically as described. In addition, without a knowledge of patient characteristics such as the PR interval at the time of image analysis, it is highly unlikely that any bias was introduced with respect to testing the hypotheses regarding the PR interval and ventricular function. Multiple scans for the same patient were analyzed at different times by raters unaware of the results of prior scans. To assess interobserver variability, two observers analyzed 20 MRI studies (10 GRE and 10 SSFP) independently and blinded to device settings.

Statistical Analysis

Data were analyzed using SAS version 9.4 (SAS Institute, Carey, NC), R version 3.6.3 (R Foundation, USA), and SPSS version 26 (SPSS, Chicago, Illinois). Baseline categorical variables were expressed as numbers and percentages. For baseline continuous variables, the median and range were reported unless otherwise stated. Overall response to CRT was determined based on the fractional change in the left ventricular end-systolic volume index (LVESVI-FC; continuous variable) post CRT (LVESVI-FC = [LVESVI post-CRT – LVESVI pre-CRT]/LVESVI pre-CRT) by CMR, such that more negative values imply a greater response. A dichotomized version of the LVESVI-FC based on a cutoff of −0.15 was also used to compare differences in patient characteristics based on a binary response indicator. Categorical variables in these two groups were compared using the Pearson's chi-squared or Fisher's exact test, while continuous variables in these two groups were compared using paired Student t-test or Wilcoxon tests. Statistical significance was established at p-value < 0.05. Pearson correlation coefficients, scatter plots, and Bland-Altman plots were used for comparisons between SSFP and GRE, and also for interobserver variability. A correlation analysis with CURE-SVD and these volumetric measurements was performed. Pairwise correlation plots with regression lines, correlation coefficients, and p-values were generated. In addition, histograms and kernel density plots were constructed, and the Kolmogorov-Smirnov test was used to test normality when indicated.

In order to provide a context for the clinical significance of MRI-derived changes in volumes and ejection fractions after CRT, the change in heart failure score, change in peak VO2, and change in VE/VCO2 slope were compared in the dichotomized groups of CRT response based on the CMR LVESV-FC criterion using a t-test or Wilcoxon test. Box plots were generated to visualize these results.

Least Absolute Shrinkage and Selection Operator (Lasso) regression (16) was used as a robust method for variable selection and variance reduction in the high-dimensional regression setting. Lasso regression was used to identify a reduced number of predictors of CMR-derived CRT response (indexed as the continuous LVESV-FC parameter) from

the following set of 26 potential covariates, which are also listed in Supplemental Figure 1: CURE-SVD, QRS duration, LGE presence, age, gender (sex), race, ischemic etiology of cardiomyopathy, diabetes mellitus, hypertension, chronic kidney disease, atrial fibrillation, prior coronary artery bypass grafting surgery, serum sodium, serum creatinine, serum hemoglobin, angiotensin converting enzyme inhibitor/angiotensin receptor blocker use, beta blocker use, loop diuretic use, statin use, systolic blood pressure, body mass index, New York Heart Association class, PR interval, QRS morphology, prior pacemaker or ICD, and scar mass by LGE. The final model was selected from the reduced set of predictors identified by the Lasso method by subsequently implementing a stepwise selection algorithm to select the model with the lowest Akaike Information Criteria.

Box-plots comparing the change in LVEF from baseline with BIVP versus LVP dichotomized by the PR interval were constructed, as synchronized LVP was hypothesized to be more beneficial with shorter PR intervals, and linear plots for each patient were also generated. Unpaired and paired t-tests were performed to assess differences in LVEF improvement based on each pacing mode. A linear mixed effects model for the change in LVEF with CRT and covariates of the PR interval, pacing mode (BIVP=1, LVP=0), and the interaction of PR interval and pacing mode was constructed. In this model, a significant p-value for the interaction term would indicate that the effect of the pacing mode on the LVEF after CRT depended on the PR interval. A similar model was constructed for the change in RVEF after CRT.

Results

Patient Characteristics

100 MRIs with 162 imaging sets (defined above) were performed in 50 patients (median age 70 years [IQR 50 to 86 years]; 48% female) before and after CRT (1 imaging set pre-CRT and 2.24 imaging sets [averaged] per patient for different pacing modes in post-CRT scans for a total of 3.24 imaging sets per patient). Patient demographics, clinical, laboratory, and baseline imaging findings are reported in Table 1. At baseline, patients had severely decreased LVEF (25.2 % [IQR 11.4 to 42.6%]) with dilated LV cavity size (median LVEDVI 118 ml/m^2 [IQR 60.9 to 299 ml/m^2] and median LVESVI 86.9 ml/m^2 [IQR 42 to 265 ml/m^2]). The median CURE-SVD at baseline was 0.58 [IQR 0.18 to 0.86]. The 22 patients with scar by LGE had a median scar mass of 16.2 g [IQR 10.2 to 32.8 g], and summary statistics for scar in all patients are provided in Table 1 CRT implantation was successful in all patients without major procedure-related complications. Follow-up scans were obtained at 6.4 ± 1.1 months post CRT implantation. During follow up (24.5 ± 9.6 months), one patient underwent left ventricular assist device implantation and one patient died with decompensated heart failure.

CMR Cine Imaging for Volumetric Analysis for Response

Table 2 describes the pre- and post-CRT CMR parameters based on RV and LV volumes. In post-CRT images, volume calculations were highly feasible despite usually minor device-related artifacts, which were present in 94% of SSFP and 75% of GRE images (examples in Supplemental Figure); however, artifact was judged to be significant in 38% of cases

with SSFP and 6% with GRE cine imaging. LVEF and RVEF measurements for SSFP and GRE correlated well pre-CRT (Figure 1A) and post-CRT (Figure 1B), with smaller volumes measured by GRE as compared with SSFP.. Interobserver analysis (CSch and AR) demonstrated excellent overall correlations for LVEF assessments by SSFP (r=0.98; p<0.001) and GRE (r=0.80, p=0.005; Figure 1C), and strong correlations for RVEF assessments by SSFP (r=0.80; p=0.01) and moderate correlation by GRE (r=0.58; p<0.01). The corresponding Bland-Altman plots demonstrated that all observations were within or close to two standard deviations from the mean.

Twenty-six patients (52%) patients showed a reduction of ≥15% in LVESVI after 6 months (LVESVI-FC ≤ −0.15) and were classified as responders based exclusively on CMR measurements for the analyses presented in Table 1 and Figure 2. As shown in Figure 2A, these patients with “CMR response” showed a greater improvement in quality-of-life score (−20.5 [IQR −14.0 to −38.0]) versus nonresponders (−2.5 [IQR −6.0 to 2.8]; p<0.001). The VE/VCO2 slope also decreased more (favorable change) in CMR responders (−2.6 [IQR −6.5 to 0] versus nonresponders (1.4 [IQR −1.1 to 3.9]; p=0.005), and the peak VO2 increased more (favorable change) in CMR responders (6.5% [IQR −4.8% to 10.9%]) versus nonresponders (−5.7% [IQR −13.6% to 4.2%]; p=0.017; Figure 2B–C).

Redaction in End-Diastolic Volumes

In order to assess biventricular reverse remodeling 6 months post CRT, LV and RV size were evaluated in diastole and independent of function. 19 patients were reprogrammed to asynchronous atrial pacing (AOO) during the post- CRT examinations. The distribution of the differences in LVEDVI and RVEDVI from the pre- CRT scan to the post CRT scan without resynchronization pacing is shown in the kernel probability density plots Figure 3. The median difference in LVEDVI after CRT was −16.3 mL [IQR −32.5 to −3.3 mL] (p=0.002), while the median difference in RVEDVI after CRT was −10.0 ml [IQR −18.6 to 2.7 mL] (p=0.16). These results are consistent with true end-diastolic volume reductions after CRT still seen even without acute resynchronization pacing.

Comparison of Outcomes Based on the CRT Pacing Mode and PR Interval

Box plots comparing unpaired LVEF changes before CRT and 6 months after CRT with BIVP versus LVP are shown in Figure 4A–B with stratification by a PR interval of 240 ms or more or less than 240 ms. Paired changes at the patient level by pacing mode and PR interval are shown in Figures 4C–D. The corresponding changes for RVEF before CRT and 6 months after CRT by pacing mode and stratified by the PR interval are shown in Figure 4E–H. LVEF and RVEF improvements were better with BIVP versus LVP in patients with a PR interval ≥ 240 ms (p=0.025 and p=0.002, respectively, based on paired t-tests). The optimal pacing mode in patients with a PR interval < 240 ms varied from patient to patient, highlighting the potential role for CMR for personalization of post-CRT programming. In mixed linear models for the change in LVEF and RVEF, the p-values for the interaction terms for PR interval*pacing mode (BIVP=1) were 0.04 and 0.0006, respectively, with a positive value for the regression coefficients, indicating that effect of the pacing mode on LVEF depended on the PR interval, with longer PR intervals favoring BIVP (Supplemental Table 1).

Comparison of CURE-SVD and Volumetric Analysis

There was an overall increase in CURE-SVD post-CRT (0.55 ± 0.18 [pre] vs 0.67 ± 0.16 [post]; p=0.015). Histograms of pre-CRT and post-CRT values (Figure 5A) and the paired differences (Figure 5B) demonstrate a rightward shift to more synchrony post-CRT and confirm feasibility of post-CRT DENSE CURE-SVD comparisons before and after CRT. A lower pre-CRT CURE- SVD (less synchrony) was associated with: 1) a greater increase in CURE-SVD (more synchrony) post-CRT ($r=-0.69$; $p<0.001$) (Figure 5C); 2) a greater increase in LVEF post-CRT ($r=-0.52$; $p<0.001$; Figure 5D); and a greater percent decrease in LVESV post-CRT ($r=-0.58$; $p<0.001$) (Figure 5E). In addition, each increase of 0.2 in the CURE-SVD post-CRT was associated with an incremental percent decrease of 18% in the LVESV post-CRT ($r=0.61$, $p<0.001$) (Figure 5E). In a multivariable linear regression analysis based on Lasso regression to identify a reduced set of optimal predictor variables (see also the Methods section), CURE-SVD at baseline was the strongest predictor of MRI-based CRT response after adjustment for other baseline patient characteristics (Supplemental Figure 1 and Supplemental Table 2). QRS duration and LGE presence were also selected as covariates in the model.

Discussion

The main finding of this study is that a CMR protocol for assessment of “CMR response” to CRT using the best cine imaging modality for each patient based on assessment of ventricular volumes, function, and strain for more than one programmed CRT setting is feasible and provides useful information for patient care. CMR provided important information regarding changes in RV and LV function from CRT, identified favorable remodeling/growth trends, and demonstrated the optimal pacing strategy.

While functional capacity (17,18), heart failure symptoms (17), and cardiac function (2) can all be used to assessed CRT response, cardiac function is frequently preferred because it assesses the most immediate impact of resynchronization pacing. While echocardiography (19,20) will continue to have a major role for this purpose because of its accessibility, favorable cost, and capacity for 3D imaging (21), echocardiographic LV volumetric assessment can be limited by several factors, including acquiring the exact 2-chamber and 4-chamber long-axis planes before and after CRT, variable quality of echocardiographic windows among patients, and challenges associated with tracing endocardial long-axis borders at end-systole and end-diastole.

CMR is considered to provide excellent assessment of LV function, RV function (22), scar (23), and strain (24). Although a CMR examination is more technically complex than an echocardiogram, CMR scanners have become increasingly accessible in current times, and CMR is increasingly the imaging modality of choice for diagnosis of cardiomyopathy etiology and scar burden. In addition, an increasing number of patients are eligible to receive macrocyclic gadolinium-based contrast agents for scar assessment based on current American College of Radiology guidelines (25). Now that these CMR scans are considered safe in nearly all patients with CRT defibrillators and pacemakers (26,27), there is an unmet need to establish scanning protocols to maximize information obtained and optimize image

quality, and this study establishes the feasibility and effectiveness of such a protocol based on assessments of multiple pacing modes in a single session.

Device algorithms to determine atrioventricular and LV-RV pacing intervals have not been associated with significant benefits in LV function using echocardiographic assessments (8). One plausible possibility for this outcome is that echocardiography may not have provided the signal-noise ratio to assess these differences. Another widely used device algorithm is LVP, in which left ventricular pacing is timed so that the wave front emanating from this electrical impulse from the LV free wall merges with conduction on the LV septum via the right bundle branch (6). While the PR interval has been presumed to be associated with the effectiveness of this algorithm relative to pacing from both the LV and RV pacing leads, echocardiography has not provided clear differentiation of the effects of this algorithm on RV and LV function. This highlights the role for CMR for personalization of the CRT pacing mode and determination of PR interval cutoffs to favor SLVP over BIVP. The rationale for stratification of the 30% of patients with a PR interval ≥ 240 ms (including patients with third degree AV block) versus patients with a PR interval < 240 ms is that BIVP is expected to be more beneficial in patients with longer PR intervals because the combination of right and left ventricular pacing with BIVP compensates for the lack of intrinsic septal conduction through the right bundle branch with long PR intervals at the time of pacing the LV free wall. The demonstration that CMR can differentiate RV and LV effects based on the PR interval for these two pacing modes also suggests that CMR could be useful to provide better signal-to-noise ratios for evaluation of the effects of other CRT pacing algorithms on LV and RV function.

The strain imaging findings are also novel, as post-CRT DENSE assessment of the CURE-SVD has not previously been compared to pre-CRT DENSE assessment of the CURE-SVD (16). The present study now extends the results of prior studies by showing that the pre-CRT CURE-SVD is also the strongest predictor of CRT response based on CMR assessments. The mechanism of this effect is more likely improvement of the post-CRT CURE-SVD with a lower pre-CRT CURE-SVD.

Limitations

Among the limitations of the present study is that not more than two to three settings were tested in a single CMR session. Of note, assessment of more settings in a single session could be feasible with increasing use of free-breathing cine imaging to acquire functional data more rapidly. In addition, CMR requires asynchronous pacing with both atrial and ventricular pacing. As a result, instead of assessing function based on atrial sensing and ventricular pacing, atrioventricular intervals are easily adjusted to account for additional atrial electrical transit time associated with atrial pacing. In addition, two of the investigators in the Imaging Core Lab (XG and KB) were initially blinded during CMR image analysis to patient characteristics and within-participant parameter values obtained across pre-CRT and post-CRT scans, but later unblinded at the time of aggregate statistical analyses. As the CMR parameter values had already been obtained prior to aggregate statistical analysis, it is very unlikely that this late unblinding significantly influenced the results reported. We also

note that larger studies, in terms of sample size, sites, and settings, would be very helpful to investigate this promising area more completely.

Conclusions

CMR evaluation with assessment of multiple pacing modes in a single session after CRT is feasible and provides useful information for patient care.

Supplementary Material

Refer to Web version on PubMed Central for supplementary material.

Acknowledgements:

The authors thank clinical research coordinators Hollis Phillips and Susan Osmanzada, and MRI technologists Jamie Weathersbee and Jose Reyes for their contributions to this work.

Funding:

Dr. Bilchick's work on this project was funded by grants R56 HL135556 (NIH), R03 HL135463 (NIH), and 17GRNT33671086 (AHA). Dr. Epstein's effort was supported by R01 HL147104. The work on this project performed by Dr. Hanson, Dr. Robinson, and Dr. Schumann was supported by NIH training grant T32 EB00384.

Relationships with Industry:

Dr. Bilchick has research grant support from Medtronic and Siemens Healthineers. Dr. Malhotra has research grant support from Biosense Webster. Dr. Darby has grant support from Medtronic and Biosense Webster. Dr. Mangrum has research grant support from Boston Scientific, CardioFocus, and St. Jude Medical. Dr. Kramer and Dr. Epstein have grant support from Siemens Healthineers.

Abbreviations:

CMR	cardiac magnetic resonance
CRT	cardiac resynchronization therapy
CURE-SVD	circumferential uniformity ratio estimate with singular value decomposition
DENSE	displacement encoding with stimulated echoes
GRE	gradient echo
ICD	implantable cardioverter defibrillator
LGE	late gadolinium enhancement
LVEF/RVEF	left/right ventricular ejection fraction
LVEDVI/RVEDVI	left/right ventricular end-diastolic volume index
LVESVI/RVESVI	left/right ventricular end-systolic volume index
SSFP	steady state free precession

References

1. Bristow MR, Saxon LA, Boehmer J et al. Cardiac-resynchronization therapy with or without an implantable defibrillator in advanced chronic heart failure. N Engl J Med 2004;350:2140–2150. [PubMed: 15152059]
2. Moss AJ, Hall WJ, Cannom DS et al. Cardiac-resynchronization therapy for the prevention of heart-failure events. N Engl J Med 2009;361:1329–1338. [PubMed: 19723701]
3. Epstein AE, DiMarco JP, Ellenbogen KA et al. 2012 ACCF/AHA/HRS focused update incorporated into the ACCF/AHA/HRS 2008 guidelines for device-based therapy of cardiac rhythm abnormalities: a report of the American College of Cardiology Foundation/American Heart Association Task Force on Practice Guidelines and the Heart Rhythm Society. J Am Coll Cardiol 2013;61:e6–75. [PubMed: 23265327]
4. Kremers MS, Hammill SC, Berul CI et al. The National ICD Registry Report: version 2.1 including leads and pediatrics for years 2010 and 2011. Heart Rhythm 2013;10:e59–65. [PubMed: 23403056]
5. Bilchick KC, Auger DA, Abdishektaei M et al. CMR DENSE and the Seattle Heart Failure Model Inform Survival and Arrhythmia Risk After CRT. JACC Cardiovasc Imaging 2020;13:924–936. [PubMed: 31864974]
6. Birnie D, Lemke B, Aonuma K et al. Clinical outcomes with synchronized left ventricular pacing: analysis of the adaptive CRT trial. Heart Rhythm 2013;10:1368–74. [PubMed: 23851059]
7. Gold MR, Birgersdotter-Green U, Singh JP et al. The relationship between ventricular electrical delay and left ventricular remodelling with cardiac resynchronization therapy. Eur Heart J 2011;32:2516–24. [PubMed: 21875862]
8. Ellenbogen KA, Gold MR, Meyer TE et al. Primary Results From the SmartDelay Determined AV Optimization: A Comparison to Other AV Delay Methods Used in Cardiac Resynchronization Therapy (SMART-AV) Trial A Randomized Trial Comparing Empirical, Echocardiography-Guided, and Algorithmic Atrioventricular Delay Programming in Cardiac Resynchronization Therapy. Circulation 2010;122:2660–2668. [PubMed: 21098426]
9. Nazarian S, Hansford R, Roguin A et al. A prospective evaluation of a protocol for magnetic resonance imaging of patients with implanted cardiac devices. Ann Intern Med 2011;155:415–24. [PubMed: 21969340]
10. Indik JH, Gimbel JR, Abe H et al. 2017 HRS expert consensus statement on magnetic resonance imaging and radiation exposure in patients with cardiovascular implantable electronic devices. Heart Rhythm 2017;14:e97–e153. [PubMed: 28502708]
11. Rashid S, Rapacchi S, Vaseghi M et al. Improved late gadolinium enhancement MR imaging for patients with implanted cardiac devices. Radiology 2014;270:269–274. [PubMed: 24086074]
12. Zhong X, Spottiswoode BS, Meyer CH, Kramer CM, Epstein FH. Imaging three-dimensional myocardial mechanics using navigator- gated volumetric spiral cine DENSE MRI. Magnetic Resonance in Medicine 2010;64:1089–1097. [PubMed: 20574967]
13. Spottiswoode BS, Zhong X, Hess A et al. Tracking myocardial motion from cine DENSE images using spatiotemporal phase unwrapping and temporal fitting. Medical Imaging, IEEE Transactions on 2007;26:15–30.
14. Spottiswoode BS, Zhong X, Lorenz CH, Mayosi BM, Meintjes EM, Epstein FH. Motionguided segmentation for cine DENSE MRI. Medical Image Analysis 2009;13:105–115. [PubMed: 18706851]
15. Ramachandran R, Chen X, Kramer CM, Epstein FH, Bilchick KC. Singular value decomposition applied to cardiac strain from MR imaging for selection of optimal cardiac resynchronization therapy candidates. Radiology 2015;275:413–20. [PubMed: 25581423]
16. Tibshirani R Regression Shrinkage and Selection via the Lasso. Journal of the Royal Statistical Society 1996;58:267–288.
17. De Marco T, Wolfel E, Feldman AM et al. Impact of cardiac resynchronization therapy on exercise performance, functional capacity, and quality of life in systolic heart failure with QRS prolongation: COMPANION trial sub-study. Journal of Cardiac Failure 2008;14:9–18. [PubMed: 18226768]

18. Arora S, Aarones M, Aakhus S et al. Peak oxygen uptake during cardiopulmonary exercise testing determines response to cardiac resynchronization therapy. J Cardiol 2012;60:228–35. [PubMed: 22542140]

19. Bilchick KC, Kuruvilla S, Hamirani YS et al. Impact of mechanical activation, scar, and electrical timing on cardiac resynchronization therapy response and clinical outcomes. Journal of the American College of Cardiology 2014;63:1657–1666. [PubMed: 24583155]

20. Chung ES, Leon AR, Tavazzi L et al. Results of the predictors of response to CRT (PROSPECT) trial. Circulation 2008;117:2608–2616. [PubMed: 18458170]

21. Takeuchi M, Jacobs A, Sugeng L et al. Assessment of left ventricular dyssynchrony with real-time 3-dimensional echocardiography: comparison with Doppler tissue imaging. J Am Soc Echocardiogr 2007;20:1321–9. [PubMed: 17764902]

22. Geva T Repaired tetralogy of Fallot: the roles of cardiovascular magnetic resonance in evaluating pathophysiology and for pulmonary valve replacement decision support. J Cardiovasc Magn Reson 2011;13:9. [PubMed: 21251297]

23. Kim RJ, Fieno DS, Parrish TB, Al E. Relationship of MRI Delayed Contrast Enhancement to Irreversible Injury, Infarct Age, and Contractile Function. Circulation 1999;100:1992–2002. [PubMed: 10556226]

24. Auger DA, Bilchick KC, Gonzalez JA et al. Imaging left-ventricular mechanical activation in heart failure patients using cine DENSE MRI: Validation and implications for cardiac resynchronization therapy. J Magn Reson Imaging 2017;46:887–896. [PubMed: 28067978]

25. ACR Manual on Contrast Media. https://www.acr.org/-/media/ACR/Files/Clinical-Resources/Contrast_Media.pdf. Accessed September 1, 2020.

26. Nazarian S, Hansford R, Rahsepar AA et al. Safety of Magnetic Resonance Imaging in Patients with Cardiac Devices. N Engl J Med 2017;377:2555–2564. [PubMed: 29281579]

27. Russo RJ, Costa HS, Silva PD et al. Assessing the Risks Associated with MRI in Patients with a Pacemaker or Defibrillator. N Engl J Med 2017;376:755–764. [PubMed: 28225684]

Clinical Perspectives

Competency in Medical Knowledge:

CRT response can be assessed effectively with CMR, which provides very high-quality data on right/left ventricular function and strain/synchrony before and after CRT.

Competency in Patient Care:

Patient care could be enhanced by CMR assessment of resynchronization pacing mode in order to personalize the CRT programming strategy. Competency in Interpersonal and Communication Skills: Results from post-CRT CMR assessments of cardiac function based on biventricular volumes and strain offers providers highly relevant data with respect to response and prognosis that could be used to formulate a plan of care.

Translational Outlook

The results of this paper offer a new paradigm with respect to the information that can be provided with post-device CMR examinations. This information could be used to design future studies that assess the effectiveness of CRT device programming and optimization.

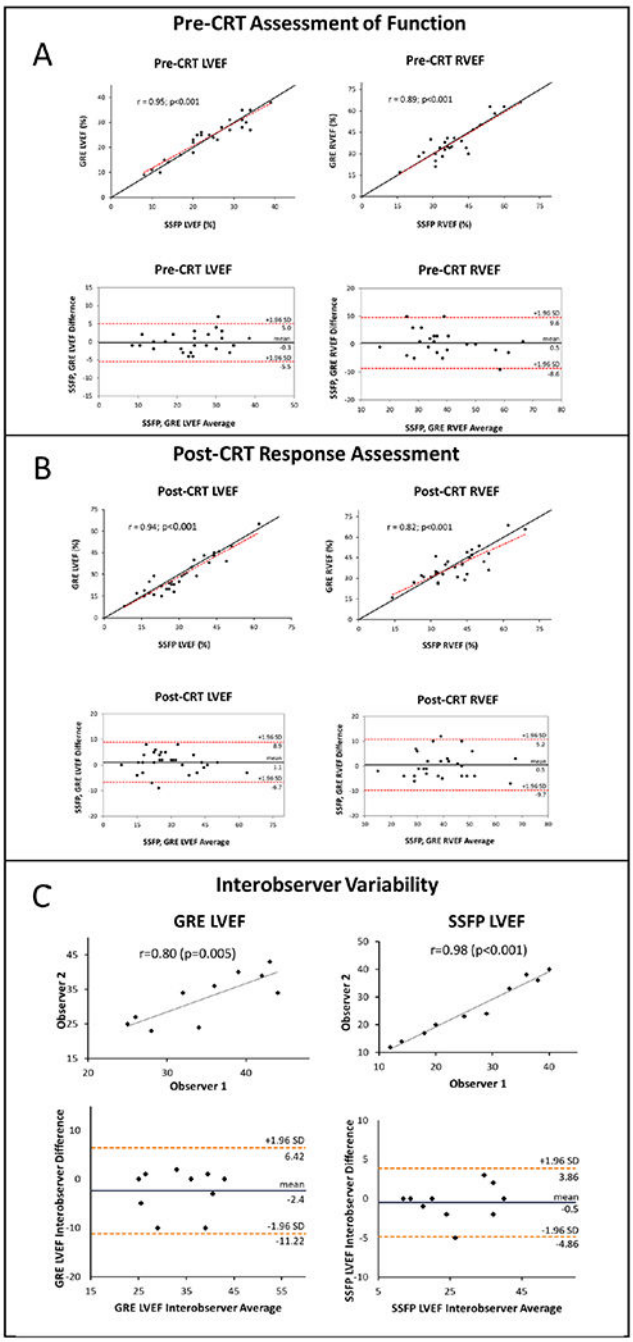

Figure 1 –. Response Assessment Based on Pre-CRT and Post-CRT CMR with Associated Interobserver Variability.

CMR assessments of baseline function with comparison of SSFP and GRE (A), response post-CRT (B), and interobserver variability for SSFP and GRE (C) are shown.

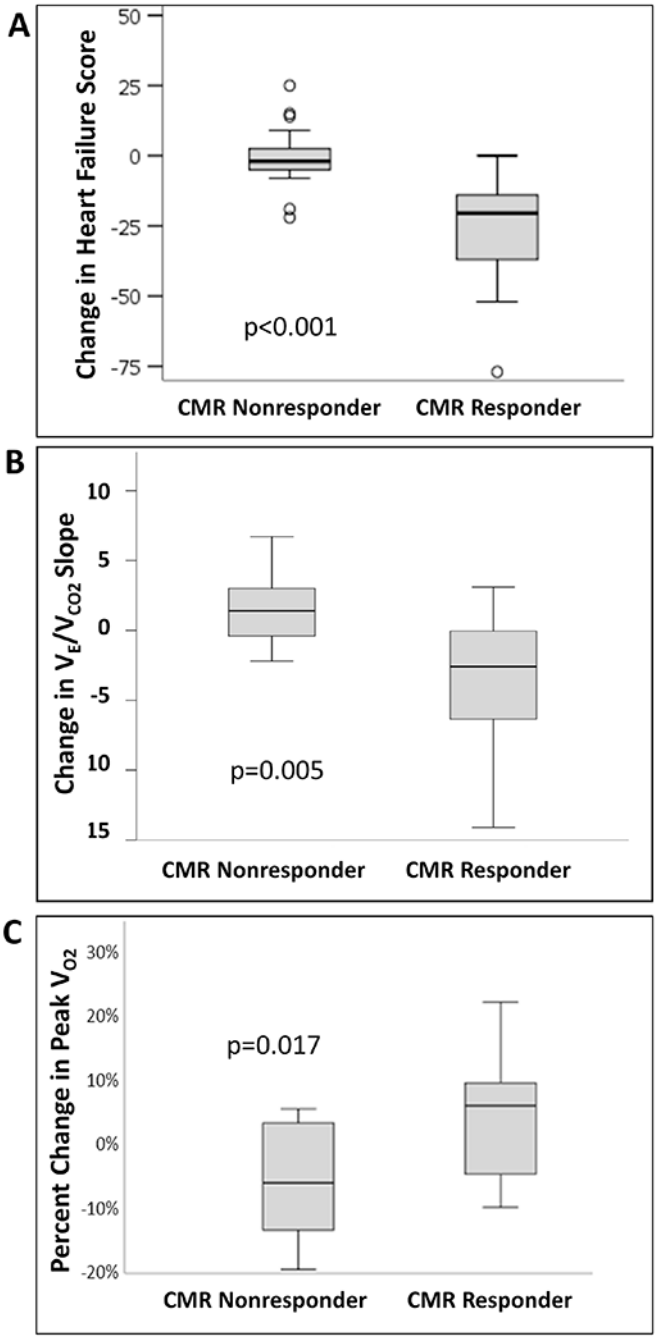

Figure 2 –. CMR Response Status Relative to Other Response Endpoints.
Endpoints include change in heart failure quality of life score (A), change in VE/VCO2 (B) and peak VO2 achieved (C).

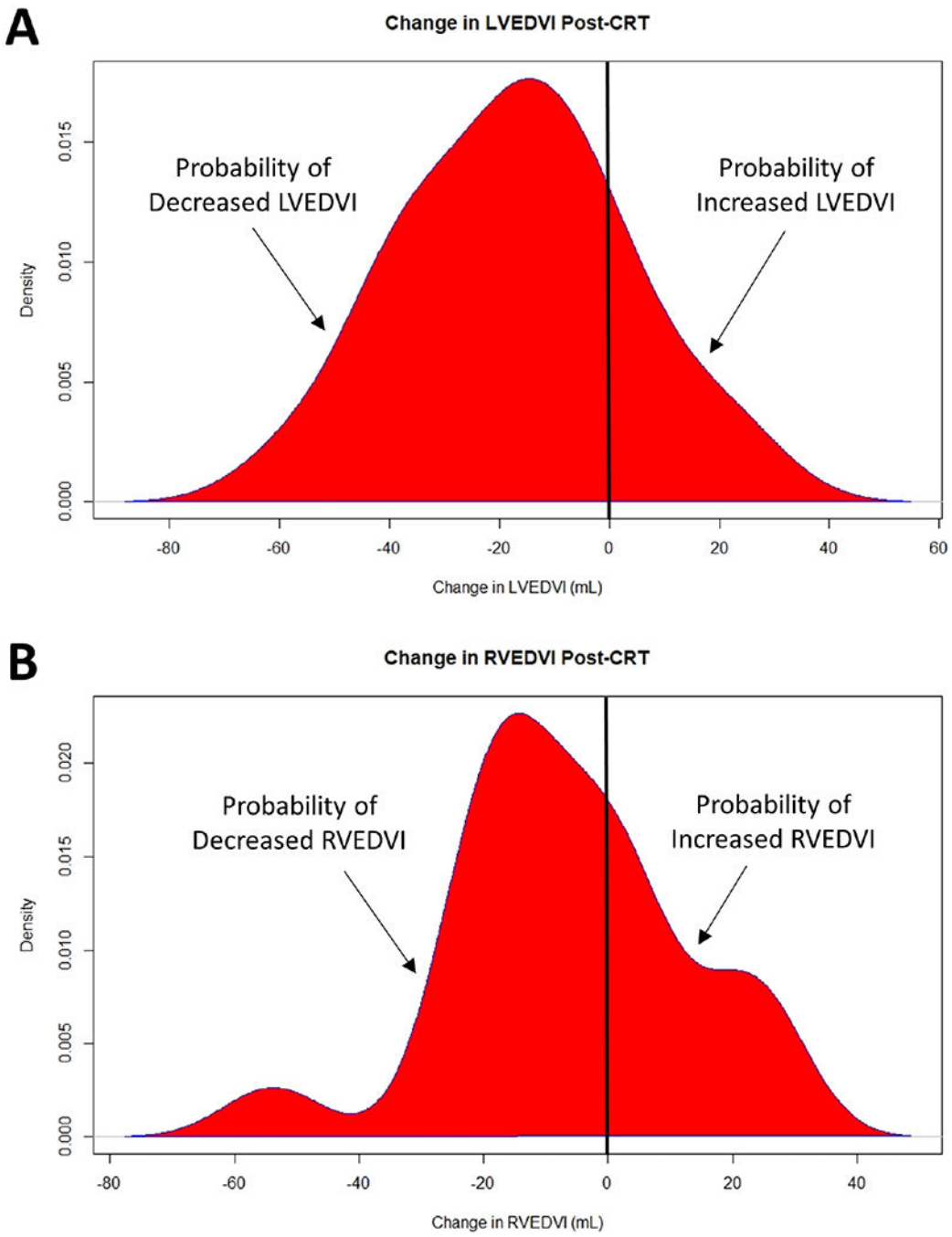

Figure 3 –. LVEDVI and RVEDVI After CRT without Resynchronization Pacing.

Shown are kernel probability density plots for the changes in LVEDVI (A) and RVEDVI (B) 6 months after CRT with asynchronous atrial pacing (AOO).

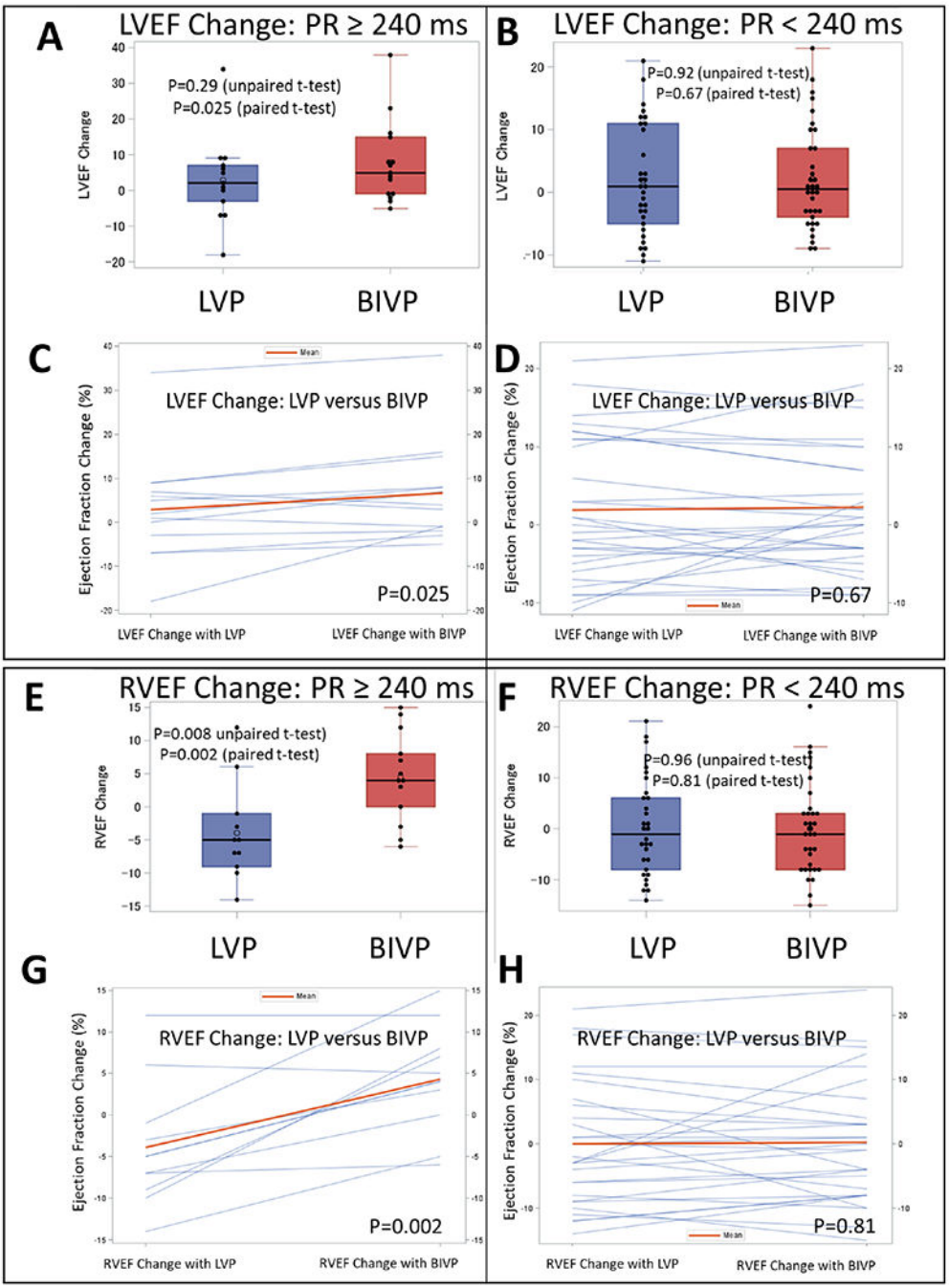

Figure 4 –. Analysis of BIVP and LVP Pacing Modes in CRT by PR Intervals.

Unpaired and paired changes in LVEF for patients with PR ≥ 240 ms (A,C) and PR < 240 ms (B,D) are shown. Corresponding changes for RVEF before and after CRT by PR interval group are shown (E-H).

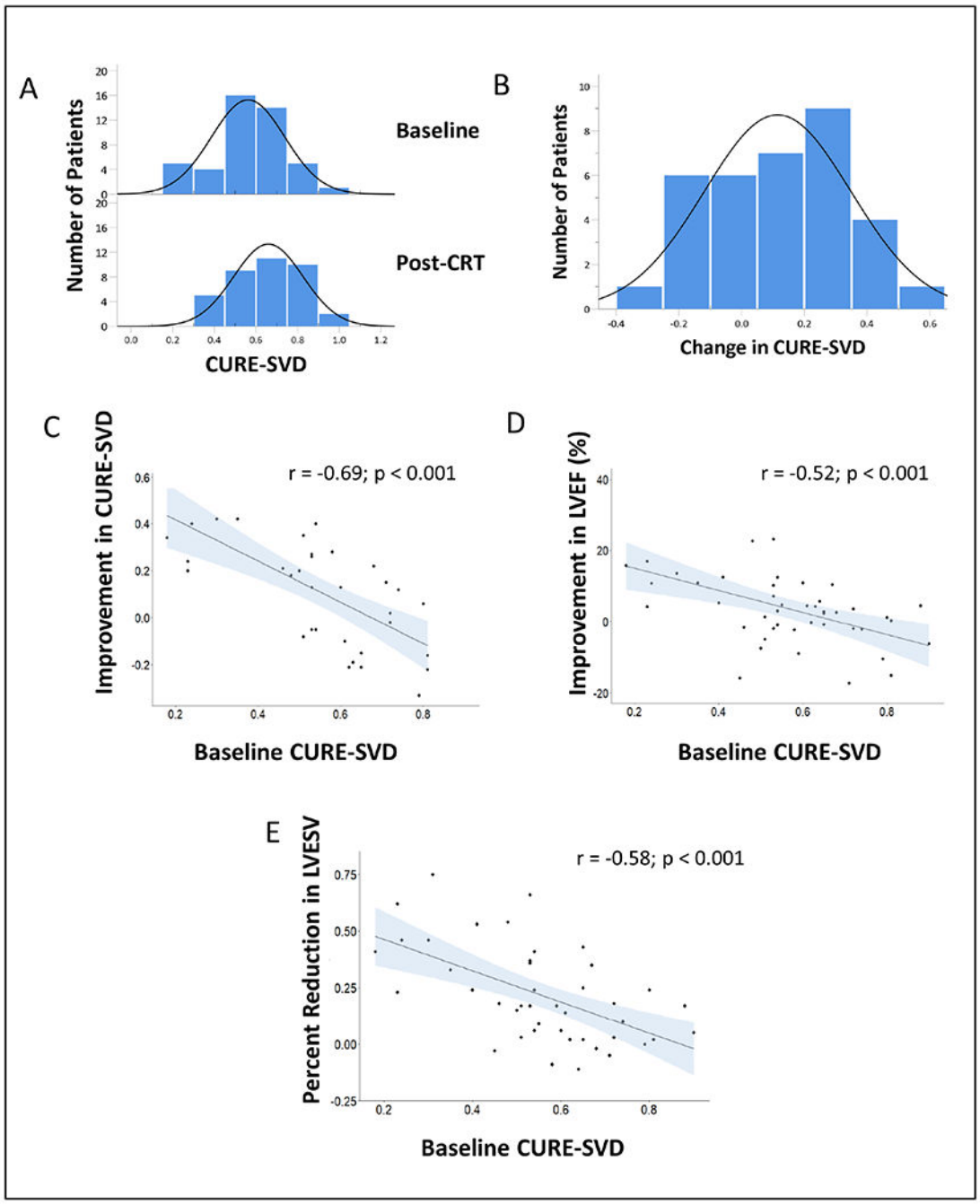

Figure 5 –. CURE-SVD Before and After CRT.

Distributions for pre- and post-CRT CURE-SVD (A) and the paired change in CURE-SVD (B) are shown. Correlation plots demonstrate improvements in the post-CRT CURE-SVD (C), post-CRT CURE-LVEF (D), and post-CRT LVESV versus the baseline CURE-SVD.

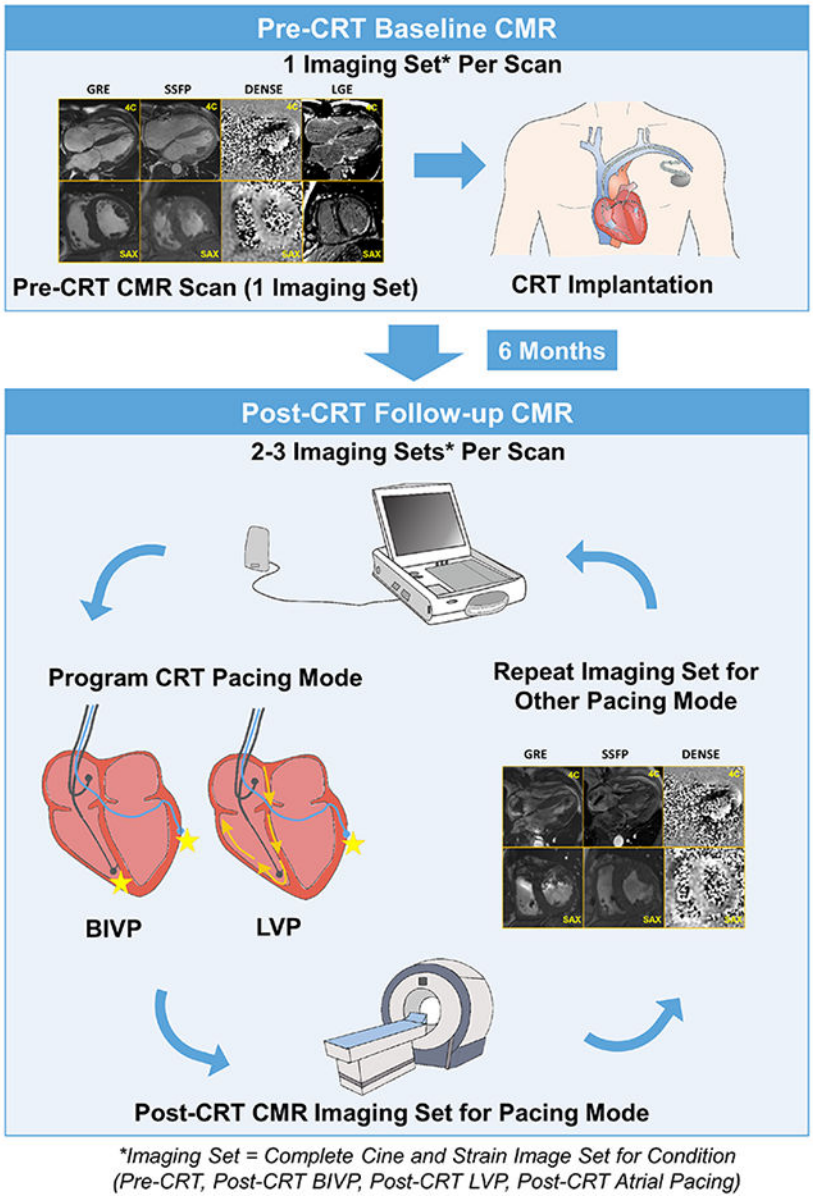

Central Illustration –. Multiple Imaging Sets in a Single CMR Examination.

The paradigm of using CMR to assess CRT response and programming strategies is illustrated. After having a CMR scan pre-CRT, patients have another CMR scan 6 months after CRT. During the post-CRT scan, multiple imaging sets with cine and strain imaging for different programmed CRT parameters are performed.

Table 1.

Baseline Characteristics

	All Patients (N=50)	CMR Responder (N=26)	CMR Nonresponder (N=24)	P-value
Age (years; median[range])	70.0 [50.0, 86.0]	70.0 [50.0, 86.0]	69.0 [55.0, 86.0]	0.46
Sex (female; no.[percent])	24 (48%)	11 (42.3%)	13 (54.2%)	0.58
Race				0.85
African American (no.[percent])	8 (16.0%)	5 (19.2%)	3 (12.5%)	
White (no.[percent])	39 (78.0%)	20 (76.9%)	19 (79.2%)	
Other (no.[percent])	3 (6.0%)	1 (3.8%)	2 (8.3%)	
Ischemic CM (no.[percent])	25 (50%)	14 (53.8%)	11 (45.8%)	0.78
Prior CABG (no.[percent])	4 (8%)	3 (11.5%)	1 (4.2%)	0.66
NYHA Heart Failure Class				0.32
Class II (no.[percent])	33 (66.0%)	15 (57.7%)	18 (75.0%)	
Class III (no.[percent])	17 (34.0%)	11 (42.3%)	6 (25.0%)	
Diabetes Mellitus (no.[percent])	16 (32%)	9 (34.6%)	7 (29.2%)	0.91
Chronic Kidney Disease (no.[percent])	21 (42%)	9 (34.6%)	12 (50.0%)	0.42
Sodium (mEq/L; median[range])	138 [128, 143]	138 [130, 142]	139 [128, 143]	0.93
Creatinine (mg/dL; median[range])	1.10 [0.600, 2.40]	1.05 [0.700, 2.30]	1.15 [0.600, 2.40]	0.15
GFR (mL/min/1.72m^2; median[range])	62.5 [28.0, 107]	65.0 [28.0, 107]	61.0 [33.0, 96.0]	0.12
Hemoglobin (g/dL; median[range])	13.0 [9.00, 16.8]	13.1 [10.0, 16.3]	12.8 [9.00, 16.8]	0.82
Medications				
Beta Blocker (no.[percent])	46 (92%)	24 (92.3%)	22 (91.7%)	1
ACE Inhibitor/ARB (no.[percent])	44 (88%)	22 (84.6%)	22 (91.7%)	0.74
Loop Diuretic Dose (mg; median[range])	40.0 [0, 160]	30.0 [0, 160]	40.0 [0, 160]	0.43
Statin (no.[percent])	33 (66%)	16 (61.5%)	17 (70.8%)	0.69
Systolic Blood Pressure (mm Hg; median[range])	120 [88.0, 148]	120 [92.0, 148]	120 [88.0, 145]	0.32
Body Mass Index (kg/m^2; median[range])	28.4 [16.5, 51.8]	27.9 [18.7, 51.8]	29.3 [16.5, 49.6]	0.87
QRS Duration (ms; median[range])	156 [120, 216]	160 [120, 200]	152 [125, 216]	0.31
QRS Morphology				0.95
LBBB (no.[percent])	31 (62.0%)	16 (61.5%)	15 (62.5%)	
RBBB (no.[percent])	12 (24.0%)	6 (23.1%)	6 (25.0%)	
Paced (no.[percent])	7 (14.0%)	4 (15.4%)	3 (12.5%)	
Upgrade Device (no.[percent])	14 (28%)	7 (26.9%)	7 (29.2%)	1
QLV Time (ms; median[range])	120 [50.0, 200]	125 [60.0, 200]	120 [50.0, 170]	0.45
CURE-SVD Dyssynchrony Parameter (median[range])	0.583 [0.177, 0.862]	0.528 [0.177, 0.862]	0.639 [0.303, 0.859]	0.047
LV End Systolic Volume Index; (mL/m^2 median[range])	86.9 [42.0, 265]	89.1 [46.5, 179]	82.9 [42.0, 265]	0.75
LV End Diastolic Volume Index (mL/m^2 median[range]);	118 [60.9, 299]	121 [75.8, 211]	114 [60.9, 299]	0.53
LV Ejection Fraction (%; median[range])	25.2 [11.4, 42.6]	25.2 [12.4, 38.7]	26.2 [11.4, 42.6]	0.83
Scar Mass (g; median[interquartile range])	0 [0, 14.8]	0 [0, 12.3]	0 [0, 15.7]	0.33
Percent Scar Volume (%)	0 [0, 11.0]	0 [0, 9.7]	0 [0, 11.4]	0.64
RV End Diastolic Volume Index (mL/m^2 median[range]);	65.1 [32.8, 251]	78.0 [39.1, 251]	61.1 [32.8, 95.2]	0.056

	All Patients (N=50)	CMR Responder (N=26)	CMR Nonresponder (N=24)	P-value
RV End Systolic Volume Index; (mL/m^2 median[range])	33.2 [14.3, 155]	44.0 [14.3, 155]	33.2 [15.0, 69.4]	0.13
RV Ejection Fraction (%; median[range])	33.3 [2.31, 65.9]	31.2 [2.31, 59.3]	34.4 [12.5, 65.9]	0.30
Baseline Peak Oxygen Output (VO2) (mL/kg/min; median[range])	14.3 [5.50, 23.7]	14.3 [6.60, 23.7]	13.7 [5.50, 21.7]	0.89
Baseline BNP (pg/mL; median[range])	368 [25.0, 3680]	264 [43.0, 3150]	438 [25.0, 3680]	0.55
Baseline Heart Failure Score; median[range])	35.0 [5.00, 94.0]	39.5 [5.00, 94.0]	25.0 [5.00, 68.0]	0.026
Survival Status				1
Alive (no.[percent])	47 (94.0%)	24 (92.3%)	23 (95.8%)	
Dead/LVAD/Tx (no.[percent])	3 (6.0%)	2 (7.7%)	1 (4.2%)	

ACE = angiotensin-converting enzyme; ARB = angiotensin receptor blocker; BNP = B-type Natriuretic Peptide; CABG = coronary artery bypass graft; CURE-SVD = circumferential uniformity ratio estimate with singular value decomposition; CM = cardiomyopathy; CMR = cardiac magnetic resonance; CRT = cardiac resynchronization therapy; GFR = Glomerular Filtration Rate; LBBB = left bundle branch block; LVAD = left ventricular assist device; NYHA = New York Heart Association; Q-LV time = the time from QRS onset on the surface ECG to the time of local LV depolarization at the location of the pacing electrode of the LV lead; RBBB = right bundle branch block; Tx = transplant

Table 2.

Summary of CMR Findings Before and After CRT

	SSFP			GRE			DENSE		
	Pre-CRT	**Post-CRT**	**p Value**	**Pre-CRT**	**Post-CRT**	**p Value**	**Pre-CRT**	**Post-CRT**	**p Value**
LVEF (%)	23.6 ± 7.7	27.8 ± 12.5	0.03	26.5 ± 8.83	2.9 ± 12	0.001			
LVESVI (mL/m^2)	98.6 ± 41.8	82.8 ±46.3	0.001	90.4 ± 46.8	72.2 ± 45.5	0.001			
LVEDVI (mL/m^2)	127.0 ± 44.1	109.4 ± 47.2	0.002	120 ± 49.7	101.6 ± 45.9	0.002			
RVEF (%)	34.6 ± 11.74	0.8 ± 6	0.02	38.4 ± 14	42.1 ± 11.7	0.02			
RVESVI (mL/m^2)	46.8 ± 20.34	1.2 ± 19.2	0.003	44.8 ± 24.4	37.8 ± 18.7	0.005			
RVEDVI (mL/m^2)	72.0 ± 24.86	2.6 ± 24.1	0.013	73 ± 32.5	65 ± 29.3	0.009			
CURE-SVD							0.55 (0.49-0.67)	0.67 (0.50-0.81)	0.015

Values are mean ± standard deviation or median (interquartile range).

CURE-SVD = circumferential uniformity ratio estimate with singular value decomposition; DENSE = displacement encoding with stimulated echoes; LVEDVI = left ventricular end-diastolic volume index; LVEF = left ventricular ejection fraction; LVESVI = left ventricular end-systolic volume index; RVEDVI = right ventricular end-diastolic volume index; RVEF = right ventricular ejection fraction; RVESVI = right ventricular end-systolic volume index; PSV = percent scar volume; SHFM-D = Seattle Heart Failure Model.